Effect of B on Crystallization of Li and Na aluminosilicates - 16323

José Marcial,[1] Joey Kabel,[2] Muad Saleh,[2] Yaqoot Shaharyar,[3] Ashutosh Goel,[3] John McCloy[1,2]
[1]Materials Science & Engineering Program, Washington State University, Pullman, WA 99164, USA
[2]School of Mechanical & Materials Engineering, Washington State University, Pullman, WA 99164, USA
[3]Department of Materials Science & Engineering, Rutgers – The State University of New Jersey, Piscataway, NJ 08854, USA

ABSTRACT

The vitrification of Hanford high-level waste (HLW) requires careful balance of glass-forming additives and nuclear waste components to maximize the waste loading but prevent adverse effects such as crystallization of aluminosilicates upon cooling in canisters. Aluminosilicate crystallization removes chemically durable glass-formers from the melt, leaving behind a residual glass that is enriched in less durable components, such as alkali and boron. In our previous work, it has been shown that the composition of the starting melt has a large influence on the phase and composition of the nucleating crystals, typically nepheline ($NaAlSiO_4$) when wastes are simultaneously high in Na and Al. Chemical partitioning allows for additional crystallization in the residual glass. Interestingly, in HLW glass the primary phases to form are those of sodium or lithium aluminosilicates despite the presence of boron, a common additive known to reduce crystallization and lower viscosity and melting point. In this work, we seek to better understand aluminosilicate crystallization in the presence of boron. Twelve glasses were prepared along the tie lines of $NaAlSiO_4$-$NaBSiO_4$ and $LiAlSiO_4$-$LiBSiO_4$. Glasses were heat-treated following a schedule that traversed the crystallization temperatures of carnegieite ($NaAlSiO_4$), nepheline, and eucryptite ($LiAlSiO_4$) as determined by thermal analysis. Samples were analyzed using X-ray diffraction (XRD), Raman spectroscopy, and differential scanning calorimetry (DSC). It was observed that Li glasses tended to crystallize at higher boron levels than Na glasses. This behavior may result from the relationship between the structure of the glass network and the structure of the resulting crystal and the relative need for atomic rearrangement prior to crystallization in the Na bearing glass.

INTRODUCTION

In vitrification, glass-forming additives are mixed with nuclear waste and charged into a melter. Glass produced through vitrification may be then poured into large steel canisters for storage in a permanent geological repository, as will be the case for glasses produced from the Waste Treatment and Immobilization Plant (WTP) in Hanford, Washington, USA. In the case of high-level waste (HLW) glasses, as the melt cools it may crystallize aluminosilicate phases depending on the thermal and chemical properties of the glass, the dimensions of the canister, and the rate of cooling. The crystallization of aluminosilicate phases has been found to be detrimental to the chemical durability. This is due to the extraction of durable $[AlO_4]^{5+}$ and $[SiO_4]^{4+}$ tetrahedra from the glass [1, 2]. The resulting glass phase that surrounds the aluminosilicate crystal, also known as the residual glass, is then enriched in less durable components (such as Na_2O and B_2O_3) and is more susceptible to corrosion [1, 2]. Besides aluminosilicate phases, HLW glasses have been shown to crystallize spinels of various compositions which are assumed to have no impact on chemical durability [1, 2]. In previous studies, we observed the presence of phosphate and silica-rich regions in particular compositions of heat treated HLW glass [3, 4]. These phases are believed to form at the glass-aluminosilicate interface and demonstrate that chemical partitioning between the glass and aluminosilicate crystal may have a large effect on the behavior of the residual melt. The impact of these additional phases on the chemical durability of HLW glass has not yet been determined.

HLW glasses may encompass large compositional spaces but are mainly comprised of alumina and silica plus oxides of boron, alkali, alkaline earth, and transition metals. Silica and boron oxide are the major glass-forming additives to HLW, hence they are present in high concentrations. Previous work has

shown that the addition of boron may help to suppress the crystallization of aluminosilicates [5]. The remaining components represent those present in HLW, where Hanford HLW is particularly high in sodium and aluminum. The presence of mixed alkali in Hanford HLW or by deliberate addition allows for the possibility of crystallization of more than one aluminosilicate phase. Due to the high sodium in Hanford HLW, nepheline ($NaAlSiO_4$) is the most common aluminosilicate phase to crystallize during cooling [6]. Nepheline is the low-temperature polymorph of the $NaAlSiO_4$ system and is a stuffed derivative of the tridymite silica structure [7]. The high-temperature polymorph of the $NaAlSiO_4$ system is carnegieite which is a stuffed derivative of the cristobalite silica structure [7]. The nominal transition temperature of nepheline to carnegieite is ~1250°C [8]. However, carnegieite is not usually observed in HLW glasses, which might be explained by the relatively low processing temperatures of HLW glass (the nominal melter operating temperature is 1150°C) and the composition of the HLW glass which usually lies in the nepheline region of the Na_2O-Al_2O_3-SiO_2 ternary diagram [9, 10]. At sufficiently high levels of lithium (> 6 wt% Li_2O), beta-eucryptite ($LiAlSiO_4$) is observed to form. Beta-eucryptite is a stuffed derivative of the beta-quartz silica structure [8]. In this work, we seek to further understand the crystallization of eucryptite and nepheline upon cooling of the melt. Raman spectroscopy was used to compare the average structures of the crystal and glass, X-ray diffraction (XRD) was used to identify the fraction of crystalline phases, and differential thermal analysis (DTA) was used to design a heat treatment schedule for all glasses.

Within HLW glass, nepheline and eucryptite often crystallize from the same melt; however, this case of crystallization is highly complex due to a "mixed alkali" effect. Understanding of this complex behavior first requires understanding of the crystallization of melts with one alkali species. To achieve this, stoichiometric glasses of $NaAlSiO_4$ and $LiAlSiO_4$ were prepared along with non-stoichiometric glasses with increasing B_2O_3 addition up to a maximum of 6.3 mol% (~7 wt%).

EXPERIMENTAL

Glasses were prepared along the tie lines of $NaAlSiO_4$-$NaBSiO_4$ and $LiAlSiO_4$-$LiBSiO_4$. Table I provides the nominal glass compositions as well as the abbreviations followed in this work. Batches were prepared by hand-mixing powdered oxides, carbonates, and hydroxides. Stoichiometric glasses ($NaAlSiO_4$ and $LiAlSiO_4$) were melted in platinum-rhodium crucibles at 1650°C for 2 hour and water-quenched. Non-stoichiometric glasses (all those containing boron) were melted in platinum-rhodium crucibles at 1500°C for 1 hour and water-quenched. Crystallization was performed by slow cooling from 1500-850°C at 10°C/min then furnace cooling from 850-330°C. This wide-temperature cooling schedule was chosen to maximize crystallization. Samples were analyzed using XRD, Raman spectroscopy, and DSC. These analytical techniques were selected because they do not present significant challenges for the measurement of Li and B as, for example, chemical analysis by electron microscopy techniques. XRD was performed using a PANalytical X'Pert Pro MPD (The Netherlands).

XRD scans were performed using a Cu-K_α X-ray source at 45 keV and 40 mA in the range of 5-100° 2θ with scan parameters: 0.002° 2θ step and 6 s dwell. For Rietveld analysis, samples were doped with 5 wt% CaF_2 internal standard and analyzed using Highscore software (PANalytical). Raman spectroscopy was performed using a Renishaw InVia Raman microscope (United Kingdom) outfitted with a Leica optical microscope. Raman spectra were collected from 1600-250 cm^{-1} using the 442 nm line of a He-Cd laser at full laser power and an exposure time of 10 s. Thermal analysis in the form of thermogravimetric analysis – differential scanning calorimetry (TGA-DSC) was performed using a Simultaneous Thermal Analyzer (STA 8000; Perkin Elmer).

TABLE I. Glass compositions and abbreviated names for this study

Abbreviation	Composition
NaB0	$NaAlSiO_4$
NaB5	$NaB_{0.05}Al_{0.95}SiO4$
NaB10	$NaB_{0.1}Al_{0.90}SiO_4$
NaB15	$NaB_{0.15}Al_{0.85}SiO_4$
NaB20	$NaB_{0.20}Al_{0.80}SiO_4$
NaB25	$NaB_{0.25}Al_{0.75}SiO_4$
LiB0	$LiAlSiO_4$
LiB5	$LiB_{0.05}Al_{0.95}SiO_4$
LiB10	$LiB_{0.1}Al_{0.90}SiO_4$
LiB15	$LiB_{0.15}Al_{0.85}SiO_4$
LiB20	$LiB_{0.20}Al_{0.80}SiO_4$
LiB25	$LiB_{0.25}Al_{0.75}SiO_4$

RESULTS

Figure 1 provides the normalized Raman spectra of glasses prepared by melt quenching at 1500°C. Figure 2 provides an example of DSC data taken upon cooling, this one for $Na_{0.75}Li_{0.25}AlSiO_4$, a boron free composition used to ensure crystallization and establish cooling temperatures for the other glasses. It can be observed that upon cooling, crystallization continued below 750°C. Based on this finding, glasses were heat treated following the schedule described in the experimental section.

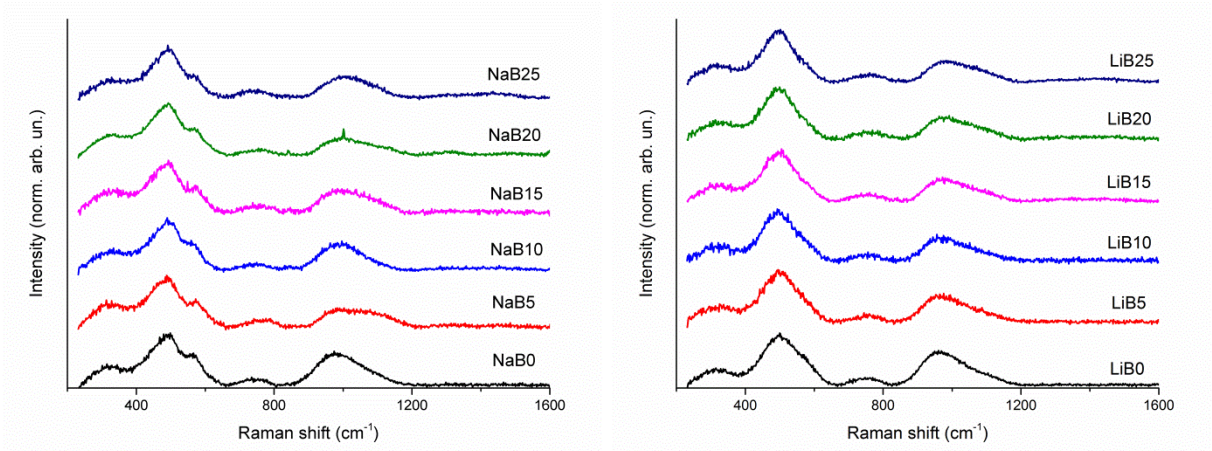

Figure 1. Normalized Raman spectra of glasses along the $NaAlSiO_4$-$NaBSiO_4$ and $LiAlSiO_4$-$LiBSiO_4$ ties

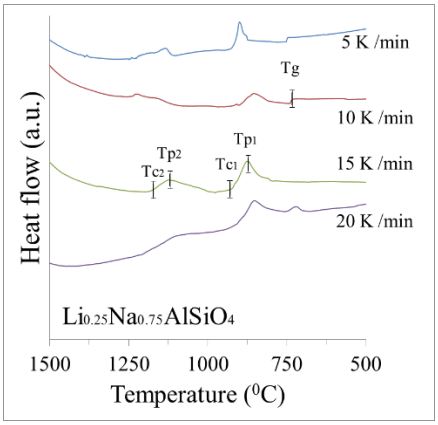

Figure 2. TGA-DTA of $Na_{0.75}Li_{0.25}AlSiO_4$ glass under various cooling rates

The Raman spectra of heat treated glasses are provided in Figure 3. Figures 4 provides Rietveld fit results for Na and Li bearing glasses. As the addition of boron increased, the relative ratio of nepheline to carnegieite after crystallization increased in NaB5 and NaB10 (structures of nepheline and carnegieite described in [11, 12, 13, 14]). After heat treatment, the relative amorphous fraction increased in Na-bearing glasses as boron concentration increased. Boron additions beyond NaB15 resulted in crystal fractions below the detectability limit of XRD. One composition, NaB5, yielded a detectable fraction of 14.6 wt% carnegieite after water quenching glass. For the Li-glass series, increasing boron addition yielded a nonlinear trend in the amorphous fraction after crystallization, and overall a much higher crystal fraction than the corresponding Na glass. The only phase detected by XRD for the Li-bearing glasses was beta-eucryptite (structure described in [15, 16, 17]). The relative fraction of beta-eucryptite reached a maximum at the LiB15 composition. Table II summarizes the international center of diffraction database (ICDD) card information for the phases fit with Rietveld.

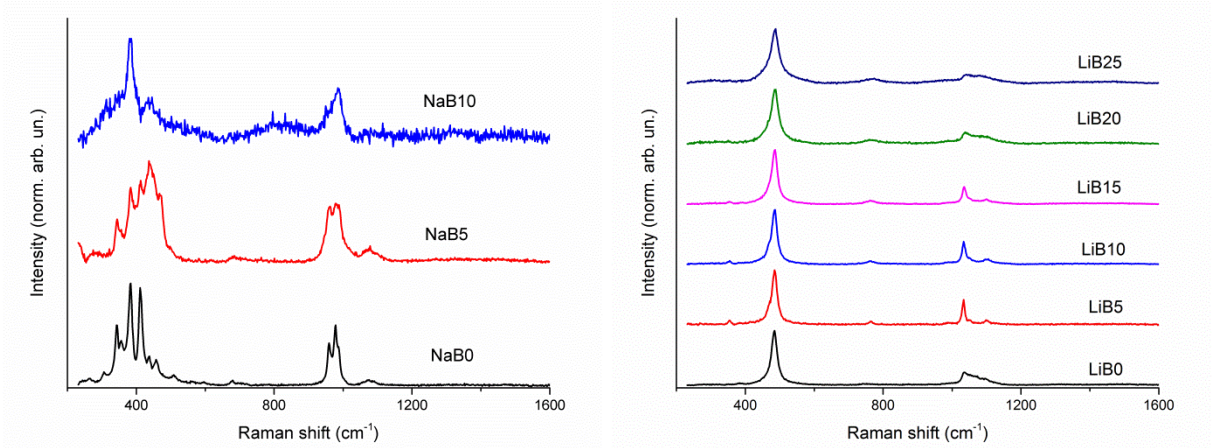

Figure 3. Normalized Raman spectra of crystallized samples along the $NaAlSiO_4$-$NaBSiO_4$ and $LiAlSiO_4$-$LiBSiO_4$ ties

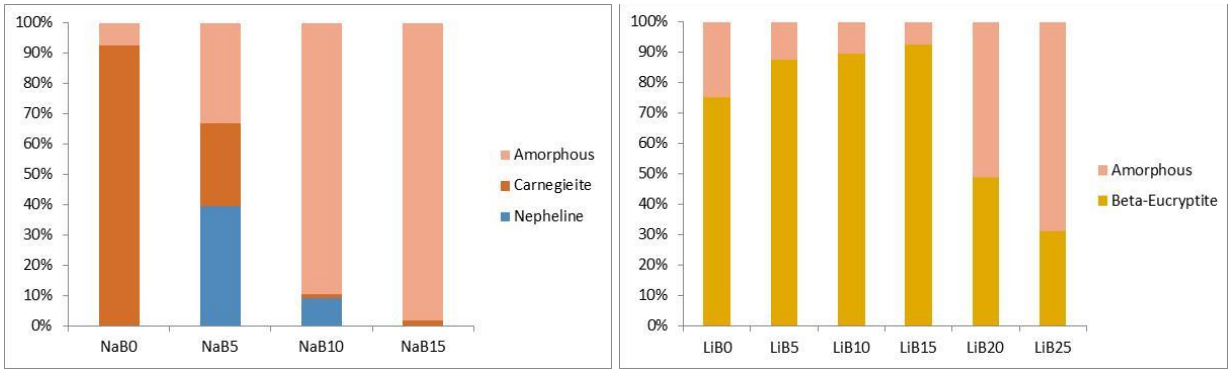

Figure 4. Rietveld analysis of crystallized samples along the $NaAlSiO_4$-$NaBSiO_4$ and $LiAlSiO_4$-$LiBSiO_4$ ties

TABLE II. Comparison of phases in heat-treated samples determined by XRD

Abbreviation	Nominal Composition	Carnegieite		Nepheline		Beta-Eucryptite	
		Wt %	Reference No.	Wt %	Reference No.	Wt %	Reference No.
NaB0	$NaAlSiO_4$	92.4	98-028-0474 [11]	--	--	--	--
NaB5	$NaB_{0.05}Al_{0.95}SiO4$	27.2	98-007-3511 [12]	39.6	98-015-5003 [13]	--	--
NaB10	$NaB_{0.1}Al_{0.90}SiO_4$	1.3	98-028-0475 [11]	9.1	98-020-0584 [14]	--	--
NaB15	$NaB_{0.15}Al_{0.85}SiO_4$	1.4	98-028-0474 [11]	--	--	--	--
NaB20	$NaB_{0.20}Al_{0.80}SiO_4$	--	--	--	--	--	--
NaB25	$NaB_{0.25}Al_{0.75}SiO_4$	--	--	--	--	--	--
LiB0	$LiAlSiO_4$	--	--	--	--	75.2	98-003-8167 [15]
LiB5	$LiB_{0.05}Al_{0.95}SiO_4$	--	--	--	--	87.4	98-003-2594 [16]
LiB10	$LiB_{0.1}Al_{0.90}SiO_4$	--	--	--	--	89.4	98-003-2594 [16]
LiB15	$LiB_{0.15}Al_{0.85}SiO_4$	--	--	--	--	92.3	98-003-2594 [16]
LiB20	$LiB_{0.20}Al_{0.80}SiO_4$	--	--	--	--	48.9	98-002-4896 [17]
LiB25	$LiB_{0.25}Al_{0.75}SiO_4$	--	--	--	--	31.1	98-002-4896 [17]

DISCUSSION

For the Na-bearing glasses, carnegieite was always present after heat treatment up to and including NaB15. In the absence of boron (that is, within the stoichiometric melt, NaB0) carnegieite crystallization was >90 wt%, despite the apparent dissimilarities between the Raman spectra of the crystallized carnegieite-containing material and the quenched glass in the ranges of 450-520 and 550-580 cm^{-1} (see Figure 5). Mineral nepheline also exhibits dissimilarities to the NaB0 glass in these ranges (Figure 5). With the addition of 1.3 mol% (1.2 wt%) B_2O_3 in the NaB5 composition, the overall crystallization is suppressed and nepheline crystallization is favored over carnegieite. This was also the case when the B_2O_3 addition was doubled in NaB10 to 2.5 mol% (2.5 wt%). Inspection of Figure 5 suggests that the Raman spectrum of NaB0 glass is more similar to nepheline than carnegieite, when comparing the relative ratios of the main peaks, though for nepheline crystal the low frequency peaks are shifted to lower wavenumbers with respect to the glass. Figures 1(a), 2(a), and 5 offer a visualization of the structural changes that the melt undergoes during crystallization, and that carnegieite undergoes as it transforms to nepheline. Further investigation is required to ascertain the mechanisms of crystallization from glass to nepheline or carnegieite. The increase in nepheline fraction as a function of boron addition can so far be explained by the increase in Si/Al ratio which shifts the composition from the carnegieite to the nepheline stability region [10]. This increase in Si/Al ratio could also explain the reduction in percent crystallinity, since the glass composition becomes more silica-rich and moves towards the nepheline discriminator limit, above which nepheline will not form [10,18].

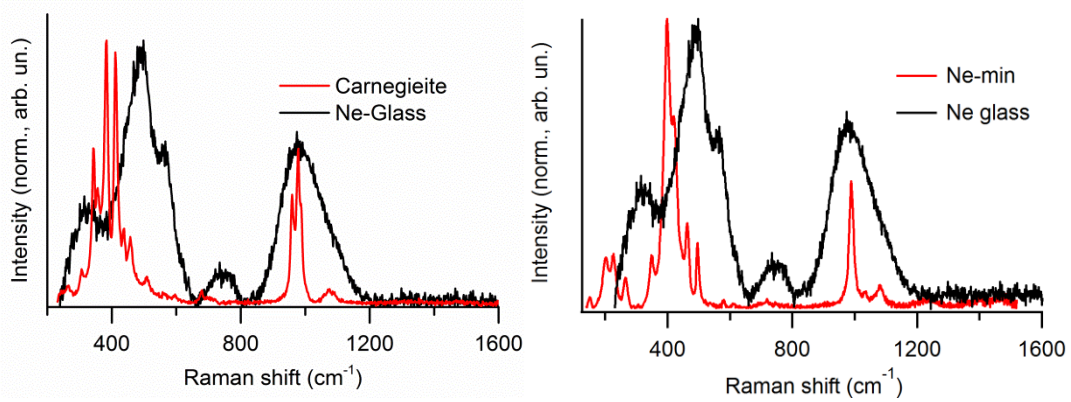

Figure 5. Comparison of normalized Raman spectra of glassy (Ne glass) and crystallized NaB0 ("carnegieite") and natural mineral nepheline (Ne-min)

The Li-bearing glasses were found to crystallize the phase beta-eucryptite. Comparison of the Raman spectra of the LiB0 glass and crystallized sample is provided in Figure 6. The similarities in peak positions at 450-520 and 1000-1200 cm^{-1} suggest that Li-bearing melts require less restructuring for crystallization than the Na-bearing melts. The Raman spectra in Figure 2 do not show a significant difference among the Li-bearing glasses to distinguish why LiB15 exhibits the highest crystalline fraction. We believe that the LiB15 composition exhibits this behavior as a result of the partitioning of boron into the residual glass. Boron is not assumed to enter the eucryptite structure and therefore forms a low-viscosity boundary layer around beta-eucryptite crystallites. We hypothesize that this low-viscosity boundary layer could function to reduce the energy required to transport an atom from the melt to the crystal surface. Evidence to support this behavior is first found in the Stokes-Einstein equation, where diffusivity is inverse to viscosity and, second, in empirically derived models for the time-temperature-transformation (TTT) diagrams of silicate melts where high viscosity significantly reduces crystal growth rates as temperatures fall below $0.7*T_E$, where T_E is the melting temperature [19]. The decreased crystalline fraction as boron addition exceeds the LiB15 composition may be attributed to a "confusion effect" as well as an increase in Si/Al ratio, described above [10]. Here the "confusion effect" may be envisioned as meaning that the boron concentration (as B^{3+} or B^{4+}) is high enough that the melt cannot make aluminosilicate rings in sufficient concentration to precipitate crystals, and rather the B^{4+} and some of the B^{3+} enter the aluminosilicate network [20]. Although the term "confusion effect" is normally applied to metallic glass systems [21], and has not yet been applied to aluminoborosilicate systems, other authors have observed similar reductions of crystallization with increasing boron addition to SiO_2-Al_2O_3-CaO systems [22]. Further structural investigation with nuclear magnetic resonance is required to fully appreciate this possibility.

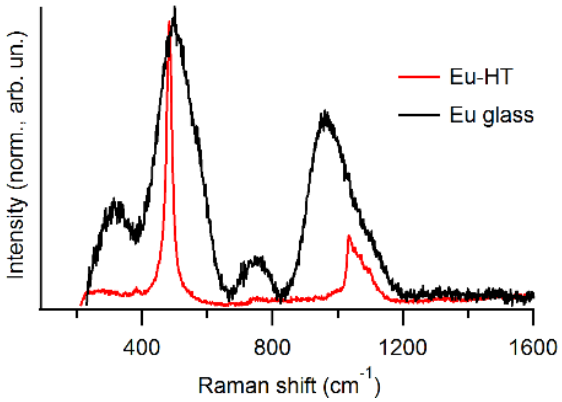

Figure 6. Comparison of Raman spectra of glassy and crystallized LiB0

For the glasses in this work, the 450-520 cm^{-1} range of the Raman spectra is associated with symmetric stretching of T-O-T linkages (where T represents tetrahedra of SiO_4, AlO_4, and possibly BO_4) in fully polymerized melts primarily comprising of six-membered rings of tetrahedra [23, 24, 25]. The range of 850-1200 cm^{-1} is associated with the antisymmetric stretching modes of T-O involving the motion of a tetrahedral cation within its oxygen cage [23, 24].

CONCLUSIONS

Previous studies have shown that aluminosilicate crystallization is detrimental to the chemical durability of HLW glasses. Chemical partitioning allows for additional crystallization in the residual glass. This work utilized Raman spectroscopy and X-ray diffraction to examine the crystallization of aluminosilicate phases in the presence of boron. Twelve glasses were prepared along the tie lines of $NaAlSiO_4$-$NaBSiO_4$ and $LiAlSiO_4$-$LiBSiO_4$. Heat-treatments of the glass were designed following the

results of thermal analysis. Li-bearing samples were found to crystallize at higher boron levels than Na-bearing samples. The Raman spectroscopy results suggest that Li-bearing melts require less restructuring during crystallization than Na-bearing samples. Observations made in the course of this study will be used in future work with aluminosilicate glasses of mixed Na and Li additions.

REFERENCES

1. C. M. JANTZEN and D.E. BICKFORD, "Leaching of Devitrified Glass Containing Simulated SRP Nuclear Waste," *Mat. Res. Soc. Proceedings*, Pittsburgh, PA, USA, 44, 135-146 (1985)
2. B.J. RILEY. P.R. HRMA, and J.A. ROSARIO, "Impact of HLW Glass Crystallinity on PCT Response," *PNNL Report*, 13491 (2001)
3. J. MARCIAL, J. MCCLOY, and O. NEILL, "Nepheline Crystallization in High-alumina High-Level Waste Glass," *Mat. Res. Soc. Proceedings*, Boston, MA, USA, 1744, Scientific Basis for Nuclear Waste Management XXXVIII, 85-91 (2014)
4. J. MARCIAL, J. CRUM, J. MCCLOY, and O. K. NEILL, "Nepheline Structural and Chemical Dependence on Melt Composition," (2015) *Am. Min.*, in press
5. H. LI, P. HRMA, J.D. VIENNA, M. QIAN, Y. SU, and D.E. SMITH, "Effects of Al_2O_3, B_2O_3, Na_2O, and SiO_2 on Nepheline Formation in Borosilicate Glasses: Chemical and Physical Correlations," *J. Non-Cryst. Solids*, 331, 202-216 (2003)
6. J.S. MCCLOY, C.P. RODRIGUEZ, C. WINDISCH, C. LESLIE, M.J. SCHWEIGER, B.J. RILEY, and J.D. VIENNA, "Alkali/Alkaline Earth Content Effects on Properties of High-Alumina Nuclear Waste Glasses," *Advances in Materials Science for Environmental and Nuclear Technology*, 63-76 (2010).
7. W.A. DEER, R.A. HOWIE, W.S. WISE, and J. ZUSSMANN, *Rock-Forming Minerals, Vol. B: Framework Silicates: Silica Minerals, Feldspathoids and the Zeolites*, 2nd Ed. The Geological Society, London (2004)
8. M.J. BUERGER, "The Stuffed Derivatives of the Silica Structures," *Am. Min.* 39 600-614 (1953)
9. A.A. KRUGER, "Advances in Glass formulations for Hanford High-Alumina, High-Iron and Enhanced Sulphate Management in HLW streams – 13000," *Proceeding for Waste Management Symposium* Phoenix, AZ (2013)
10. J. MCCLOY, N. WASHTON, P. GASSMAN, J. MARCIAL, J. WEAVER, and R. KUKKADAPU, "Nepheline Crystallization in Boron-Rich Alumino-Silicate Glasses as Investigated by Multi-Nulcear NMR, Raman, and Mossbauer Spectrscopies," *J. Non-Cryst. Solids*, 409, 149-165 (2015)
11. S.R. PALETHORPE, A. MELNITCHENKO, R.L. WITHERS, and J.G. THOMPSON. *Acta Crystallographica*, Section B: Structural Science 54, 531 - 546, (1998)
12. J.G. THOMPSON, and R.L. WITHERS, *Acta Crystallographica*, Section B: Structural Science. 49, 614 - 626, (1993)
13. S. MACURA, S. MARKOVIC, P. VULIC, V. DONDUR, and R. DIMITRIJEVIC. *Journal of Physics and Chemistry of Solids*, 65, 1623 - 1633, (2004)
14. W.M. THOMAS and W.A. DOLLASE. *Contributions to Mineralogy and Petrology*, 66, 311-318, (1978)
15. H. G. F. WINKLER, *Golden Book of Phase Transitions, Wroclaw*, 1, 1-123, (2002).
16. G. HEGER and H. GUTH, *Fast Ion Transports in Solids, Elektrodes, Elektrolytes*, 1979, 499 - 502, (1979)
17. L. CHI-TANG, *Zeitschrift fuer Kristallographie, Kristallogeometrie, Kristallphysik, Kristallchemi*, 127, 327-348, (1968)
18. LI, H., J.D. VIENNA, P. HRMA, D.E. SMITH, and M.J. SCHWEIGER, "Nepheline precipitation in high-level waste glasses: compositional effects and impact on the waste form acceptability," *Mat. Res. Soc. Preceedings*, Pittsburgh, PA, USA, 465, Scientific Basis for Nuclear Waste Management XX, Materials Research Society, 261-268 (1997).
19. D. UHLMANN, "Kinetics of Glass Formation and Devitrification Behavior," *Journal of Physique Colloques*, 43, 175-190 (1982)
20. E.M. PIERCE, L.R. REED, W.J. SHAW, B.P. MCGRAIL, J.P. ICENHOWER, C.F. WINDISCH, E.A. CORDOVA, and J. BROADY, "Experimental determination of the effect of the ratio of B/Al on glass dissolution along the nepheline ($NaAlSiO_4$) – malinkoite ($NaBSiO_4$) join," *Geochimica et Cosmochimica Acta*, 74, 2634-2654 (2010)
21. E. AXINTE, "Metallic glasses from "alchemy" to pure science: Present and future design, processing and applications of glassy metals," *Materials and Design* 35, 518-556 (2012)

22. M. HILLERS, G. MATSEN, E. VERON, M. DUTREILH-COLAS, and A. DOUY, "Application of *in situ* high-temperature techniques to investigate the effect of B_2O_3 on the crystallization behavior of aluminosilicate E-glass," *J. Am. Ceram. Soc.*, 90, 720-726 (2007)
23. D.W. MATSON, S.K. SHARMA, and J.A. PHILPOTTS, "Raman spectra of some tectosilicates and of glasses along the orthoclase-anorthite and nepheline-anorthite joins," *Am. Min.*, 71 694–704 (1986)
24. C.M.S.DAN SYKES, "Melt structure in the system nepheline-diopside," *Journal of Geophysical Research*, 951, 15745–15749 (1990).
25. D. MANARA, A. GRANDJEAN, and D. NEUVILLE, "Advances in understanding the structure of borosilicate glasses: A Raman spectroscopy study," *Am. Min.*, 94, 777–784 (2009)

ACKNOWLEDGMENTS

This research was supported by the Department of Energy's Waste Treatment and Immobilization Plant Federal Project Office, contract number DE-EM002904, under the direction of Dr. Albert A. Kruger. The authors would like to thank Dr. Yi Gu and Xin Tao for granting access to their Raman Spectrometer.